JOURNAL OF MATERIALS SCIENCE **35** (2000) 4673–4683

# A new method for assessing the mean grain size of polycrystalline materials using ultrasonic NDE

L. R. BOTVINA
*Institute of Metallurgy, Russian Academy of Sciences, Moscow, Russia*

L. J. FRADKIN, B. BRIDGE
*School of Electrical, Electronic and Information Engineering, South Bank University, London SE1 0AA, UK*
*E-mail: fradkil@sbu.ac.uk*

We re-analyze published data on ultrasonic inspection of a number of pure metals and alloys involving a range of mean grain sizes (from 0.0125 mm to 0.3 mm). We show that they may be described by one master curve graph consisting mainly of two distinct but parallel linear segments. This means that our presentation clusters the data under study into two distinct groups, each chracterized by its own generalized material constant. The slope of the segments suggests the predominance of scattering other than Rayleigh's, since it is consistent with the second power law rather than the fourth. We argue that the attenuation is likely to be due to multiple scattering, particularly since our generalized material constants seem to be similar to the published stochastic scattering factors. The master curve graph suggests a new fast and simple method for assessing the mean grain size which may be carried out without recourse to standard specimens or measurements other than those routinely carried out during ultrasonic inspection. As the range of materials and grain sizes are in extensive use in industry the simple schedule proposed should prove of substantial use in practical material evaluation and production process control. 

## 1. Introduction

It is accepted that the same features of microstructure that dominate attenuation of ultrasonic waves also determine mechanical properties of industrial materials. For example, in polycrystalline metals the grain size greatly influences both ultrasonic attenuation [1–4] and material strength, ductility, toughness and formability [5–7]. Since ultrasonic inspection is less expensive than the destructive tests required to assess mechanical properties many analytical and experimental studies have been directed at establishing whether and how features of microstructure may be inferred from ultrasonic inspection data. As a result, a number of dimensionless parameters have been proposed in the non-destructive evaluation (NDE) literature to describe various attenuation regimes. These regimes are usually determined by the magnitude of the ratio of the ultrasonic wavelength to the mean size of inhomogeneity. There appears to be a broad consensus on what the regimes are, but the thresholds which separate them appear to be material dependent and what makes the traditional models even less practicable, they allow identification of the mean grain size only if some elusive material constants are known. Indeed, in most cases these cannot be estimated analytically and are difficult to measure. In the present paper we analyze published data pertaining to different pure metals and alloys and arrive at a somewhat unorthodox combination of variables, one involving the rate of the attenuation change with frequency. This choice of variables allows most published data to be plotted on one master curve: This particular curve had been arrived at via exploratory data analysis which involved testing various *equivalent* versions of the piece-wise power law hypothesis. It allows a *convenient* data visualisation, i.e. reduction in visual data spread, and thus leads to smaller variance of residuals. The master curve could be used to estimate the mean size of the metal grain in a fast and inexpensive manner.

Apart from being of immense value in quality control, the universal relationships between the mean grain size and ultrasonic parameters are of fundamental interest. For example, it is well known that if a process is self-similar, that is if a quantitative relationship between its characteristic variables is the same over a wide range of scales, then it is of a power-type [8]. For this reason, when a power-type relationship has been found, and the presence of *two* such relationships, one for each particular group of metals is confirmed below, it is current scientific practice to ascertain experimentally whether self-similarity is present as well. Even if it is not experiments of this kind throw additional light on the physical nature of the relationship.

## 2. Background

Attenuation $\alpha$ is a widely used ultrasonic parameter. It is measured in nepers/cm (or db/m) and represents a relative energy loss experienced by an ultrasonic plane wave per unit length of a solid sample. Many authors believe that in polycrystalline materials attenuation is due mainly to *scattering* (reorientation and mode conversion of energy) by the grains [1, 2] and precipitates [9]. Scattering results from interaction with material defects comparable to one wavelength in size, e.g. grain boundaries. For this reason, scattering depends on size, shape, orientation and anisotropy of the grains, the structure and thickness of their boundaries as well as chemistry, e.g. the presence of alloying materials or deposits. The standard assumptions used when modeling grain scattering are:

(i) the discontinuity of the grain boundary is of elastic nature, so that there is no discontinuity of density;
(ii) an individual grain scatters as a sphere/cube/cylinder;
(iii) the grains are randomly located and randomly oriented, so that the bulk of material is elastically homogeneous and isotropic;
(iv) the number of grains is large;
(v) the scatter from individual grains is not coherent.

Using these assumptions, three major scattering regimes have been identified (other, bridging, regimes are occasionally mentioned as well). Their description in terms of dimensionless variables is presented in Table I. We use standard notations: $D$ is the diameter of sphere equivalent to mean grain size, $\lambda = v/f$ is the ultrasound wave length, $f$ is the ultrasound frequency and $v$ is the speed of sound in the inspected material.

The first regime in which the wave length is much larger than the grain size is called *Rayleigh* after Lord Rayleigh [10] who first described scatter of waves with a large wavelength by a small sphere. The application of Rayleigh's formula obviously involves an additional assumption:

(vi) the scattered energy is sufficiently small, so that multiple scattering effects may be neglected.

The second regime is called *stochastic* to indicate that when the wave length is comparable to the grain size the Huygens (spherical) wavelets which emanate from the neighboring points on the incident plane wave front travel through randomly oriented individual grains. Thus they change their velocity in a random manner and arrive at the receiver with randomly distributed phases. The third regime is called *diffusion* to indicate that when the wave length is small a cycle of the ultrasound wave scatters from many grain boundaries within a unit distance of travel. Note that the stochastic scattering and diffusion models do not rely on the single scattering assumption (vi). In the Rayleigh regime the scattering term is proportional to *the fourth power* of $f$ and $D$ [1–4, 11] (the third power if the scatterers are cylindrical - [12]), in the stochastic regime to the *second power* of $f$ and $D$ [11, 13] and in the diffusion regime it is *a constant* [1, 2]. A simple justification of these relationships based on dimensional arguments is presented in [14].

The agreement between theory and experiment is considered to be moderate, nevertheless the early work [1, 2, 13, 15] in relatively pure materials is taken to provide qualitative substantiation to the existence of loss mechanisms described in Table I. In [3] and [4] the theoretical analysis of [16] was adapted to produce quantitative confirmation for the Rayleigh and stochastic regimes by taking into consideration losses due to the mode conversion at the grain boundaries. It was concluded that similar description could be adopted for characterizing steel alloys, even though their material constants could not be estimated analytically. This is not entirely consistent with the findings in [17] where it was noted that when experimenting with steel the $f^2$–term often dominates.

The difficulties associated with interpreting attenuation-frequency experiments in terms of the scattering regimes have been highlighted in [18–23]. Allowances that have to be made to take into account the effect of the boundary conditions and the energy absorbed by the transducer from each succeeding echo are described in [18]. In [19, 20, 22, 23] it is pointed out that this model fails at lower frequencies where beam spread losses become prominent. It is argued in [22] that in some cases, the frequency-attenuation curves can be corrected for beam spread by extrapolating their high frequency portions - if these involve the Rayleigh or stochastic regimes. In [21] attention is drawn to further problems associated with the presence of *absorption, grain size distribution* and *grain substructure*.

In general, *absorption* (conversion of acoustic energy into heat) can be linked to anelastic behaviour of solids [24] which is due to inhomogeneities on a much finer scale than $D$, such as magnetic domain motion and dislocations and interstitials. The absorption effects can be taken into account to extend Table I - see Table II.

TABLE I Three major scattering regimes. $A_r$, $A_s$ and $A_d$ are scattering coefficients characterizing anisotropy and the average change in elastic properties between grains

| Scattering regime | Validity range | $D\alpha$ |
|---|---|---|
| Rayleigh | $\frac{D}{\lambda} \ll 1$ | $A_r \frac{D^4}{\lambda^4}$ |
| Stochastic | $\frac{D}{\lambda} \approx 1$ | $A_s \frac{D^2}{\lambda^2}$ |
| Diffusion | $\frac{D}{\lambda} \gg 1$ | $A_d$ |

TABLE II Standard attenuation regimes. $A_1$, $A_2$, $A_3$, $n$ and $m$ - material constants, $n \leq 2$, $D_1$ and $D_2$ - characteristic scales different to $D$

| Attenuation regime | Validity range | $D\alpha$ |
|---|---|---|
| Large wavelength | $\frac{D}{\lambda} \ll 1$ | $A_1 \frac{D}{\lambda} + A_2 \frac{DD_1}{\lambda^2} + A_r \frac{D^4}{\lambda^4}$ |
| Intermediate wavelength | $\frac{D}{\lambda} \approx 1$ | $A_1 \frac{D}{\lambda} + A_2 \frac{DD_1}{\lambda^2} + A_s \frac{D^2}{\lambda^2}$ |
| Small wavelength | $\frac{D}{\lambda} \gg 1$ | $A_1 \frac{D}{\lambda} + A_2 \frac{DD_1}{\lambda^2} + A_3 \frac{D}{D_3} \frac{D_2^n}{\lambda^n} + A_d$ |

All three models in Table II involve the magnetic (hysteretic) absorption term which is proportional to $f(D/\lambda)$ [25–28], and dislocation absorption term which is proportional to $f^2(DD_1/\lambda^2)$ [23] and [29–31]. Here $D_1$ is another characteristic scale, the mean dislocation loop length in a unit volume. Note that the $f^2$-term could be also due to molecular relaxation of frequency above the experimental range [32] or to magnetic wall effects [33, 34]. The small wavelength equation contains an additional term which is due to thermoelastic loss and is proportional to $f^{1/2}((D_2/\lambda)^{1/2})$ according to [35, 36] or $f^2$ according to [37] where this claim is not justified. Here $D_2$ is yet another characteristic scale - this time of thermal diffusion.

These days absorption can be obtained directly, for example by using a technique based on the infrared detection of the heat produced by ultrasound [38–40]. Eliminating its contribution allows one to investigate scattering regimes with greater precision. However, such elimination has not been done in the past and there are still a lot of data around with both scattering and absorption present. It is claimed in [22] that it is possible to use *Roney's generalized attenuation theory*: Thus, the relationship between attenuation, frequency and mean grain size can be expressed in terms of dimensionless variables $D\alpha$ and $\pi D/\lambda$; the attenuation loss in the entire megahertz frequency range can be accounted for using just two constants, a hysteretic and a scattering coefficient [41]. The hysteretic constant is well established and its experimental determination can be accomplished by low frequency internal friction measurement (*ibid*). This result supersedes that of [42] which is based on an assumed autocorrelation function for the material discontinuity and could be used to bridge the Rayleigh and stochastic regime. It is proposed in [22] to treat the other constant not only as characterizing the material anisotropy (as in [41]) but as a more general parameter dependent on grain boundary characteristics as well as mode conversion factors. Of course, this theory (at least in its original form) does not allow for other absorption mechanisms.

The *grain distribution* problem cannot be solved by an experimental elimination procedure. Its magnitude seems to have been underestimated in [1, 2]. For example, it is remarked in [15] that no special annealing procedures had been used to prepare the corresponding samples, and thus the estimate of the relative error in $D$ as $\approx\pm 5$–10% seems unrealistic. Numerical data and discussion of how the diameter of the equivalent sphere is related to the mean size as estimated from metallographic studies, that is photo-micrographs can be found in [11]: In the Rayleigh regime the mean grain size is evaluated by taking the distribution of sizes into account, but in the stochastic regime the direct use of the mean grain size is usually advocated. This may be due to the fact that in the stochastic regime the variability in grain sizes is less important. In [43] and [44] ultrasonic attenuation has been modeled by combining Roney's generalized theory and the assumption that grain sizes are distributed according to a power law. It has been concluded that while the Rayleigh and diffusion regimes still hold, in the intermediate frequency regime, where $D_{\min} \le \lambda \le D_{\max}$ ($D_{\min}$ and $D_{\max}$ being the minimum and maximum grain sizes respectively), the attenuation varies with wavelength according to the same power law which characterizes the grain size distribution. Later it has been shown in [44] that under reasonable assumptions inverse techniques may be used to estimate grain size distribution from attenuation data. We are not aware of any models which take into account the influence of *the grain substructure* on ultrasonic attenuation.

Thus, there is a lot of controversy in the literature as to the significance and functional dependene of various absorption mechanisms as well as to the limits of applicability of thresholds between different attenuation regimes. It is also clear that the quality of the published data is often in question. Nevertheless, we would suggest that the approach of [22] is fruitful and be generalized further by assuming that attenuation-frequency data can be described in terms of dimensionless parameters related by a power law and a *generalized material constant* dependent on the whole multitude of microstructural parameters.

To be more precise, let use assume that $\alpha$ is a function of several, parameters, D, $f$ and $v$. Then it follows from the first principles that $R \equiv D\alpha$, a dimensionless attenuation, is a function of the dimensionless parameter $D/\lambda$,

$$D\alpha = R\left(\frac{D}{\lambda}\right). \tag{1}$$

The existence of other independent dimensionless parameters will be addressed below.

Let us now introduce a *hypothesis* that this dependence is in the form of a piece-wise power law, so that there are several $D/\lambda$-regimes, where one power law dominates and we have

$$D\alpha = A\left(\frac{D}{\lambda}\right)^{\nu_1}, \tag{2}$$

with $A$ and $\nu_1$ constants which differ from one regime to the next, and $A$ a generalized material constant of the type discussed above. To test (2) we plot $D\alpha$ versus $D/\lambda$ on the log-log scale, where base 10 is implied. It can be also tested by differentiating $\alpha$ with respect to $\lambda^{-1}$ to obtain

$$v\frac{\mathrm{d}\alpha}{\mathrm{d}f} = A\nu_1\left(\frac{D}{\lambda}\right)^{\nu_1-1} \tag{3}$$

and then plotting $v\mathrm{d}\alpha/\mathrm{d}f$ versus $D/\lambda$ on the log-log scale. It is well known that derivatives are sensitive to experimental errors and thus are less reliable than the data that have not been differentiated. However, this can be taken into account in data and error analysis, and also, although not available to us, $\mathrm{d}\alpha/\mathrm{d}f$ happens to be a variable which is measured more accurately in frequency/attenuation experiments than $\alpha$: The form of the LHS in (3) has been chosen to reflect this fact. The variable $\frac{\mathrm{d}\alpha}{\mathrm{d}f}$ had been used for attenuation data analysis previously [15, 45]. Finally, we note that substituting (2) into (3) gives

$$v\frac{\mathrm{d}\alpha}{\mathrm{d}f} = A^{1/\nu_1}\nu_1(D\alpha)^{(\nu_1-1)/\nu_1}. \tag{4}$$

This suggests a yet another form of the piece-wise power law hypothesis,

$$v\frac{\mathrm{d}\alpha}{\mathrm{d}f} = A_0(D\alpha)^{\nu_0}, \tag{5}$$

where different regimes differ only by the values of constants $A_0 = A^{1/\nu_1}\nu_1$ and $\nu_0 = (\nu_1 - 1)/\nu_1$. This form proves of interest below. It is important to realise that if the hypothesis (2) is correct, then both hypotheses (3) and (5) are equivalent to it. On the other hand, in some situations, say if $\alpha$ contains extra terms, the other two hypotheses might produce a smaller or more normally distributed model error. This realisation lies behind the idea of exploratory data analysis routinely used in System Identification (a part of control theory) at the stage of Model Structure Identification (e.g. [46]). Different equations (structures) are compared in order to find the one giving the most advantageous residuals.

As we have already mentioned, the above considerations apply even when there are more than two independent parameters. Indeed, let there be, say, two characteristic scales, $D$ and $D_1$. Then there exists a function $R$, such that

$$D\alpha = R\left(\frac{D_1}{D}, \frac{fD}{v}\right). \tag{6}$$

If plotting $R$ on the log-log scale versus one of its dimensionless parameters, say, $D/\lambda$ produces a universal piece-wise straight line, then the piece-wise power law is confirmed for $D/\lambda$ and other parameters may be neglected. If this exercise produces a host of parallel straight lines, then the power-law assumption is correct for $D/\lambda$, but dependence on $D_1/D$ should be investigated further. If no straight line appears, as far as $D/\lambda$ is concerned the power-law hypothesis is invalidated.

Let us now analyze published data and suggest a new approach for estimation of the mean grain size from the frequency/attenuation measurements. We will show that this approach appears to be more reliable and easier to implement than other widely accepted methods.

## 3. Exploratory data analysis

We undertook a thorough literature search and analyzed all the relevant data we uncovered. The data are not necessarily of the highest quality, so we endeavour to use only robust statistical measures insensitive to error distribution (such as means as opposed to standard deviations) and generally rely on the the approach of Exploratory Data Analysis and System Identification as developed for modeling engineering ill-defined systems rather than well executed physical experiments. The types of materials studied, the corresponding references and conclusions made by the original authors are all summarized in Table III. It is assumed throughout that during the experiments the only structure parameter that had been varied was the mean grain size.

To simplify the presentation we group the experiments under consideration into three different classes:

(1) attenuation of *longitudinal* ultrasonic waves in the *steel* rods,

TABLE III Typical attenuation/frequency/mean grain size experiments and conclusions concerning attenuation regimes and thresholds

| Materials | Refs | Suggested thresholds and mechanisms |
|---|---|---|
| Aluminium, Magnesium | [1], [2] | $D/\lambda < 1/3$ - Rayleigh scattering and magnetic hysteresis<br>$D/\lambda > 3$ - diffusion scattering |
| Iron, Copper, Magnesium | [3] | $D/\lambda < 1/10$ - Rayleigh scattering and magnetic hysteresis |
| Steels 12, 15 & 40 | [4] | $1/10 < D/\lambda < 1/4$ - stochastic scattering |
| Steels 31440, 4150 | [12] | $D/\lambda < 1/2T_1$ - Rayleigh scattering<br>$1/3 < D/\lambda < 3$ - stochastic scattering |
| Steel 46 | [48] | $D/\lambda < 1/4\pi$ - Rayleigh scattering |
| Steel NiMoV | [47] | $D/\lambda < 1/30$ - Rayleigh scattering<br>$1/7 < D/\lambda < 1/2$ - stochastic scattering |

(2) attenuation of *longitudinal* ultrasonic waves in the rods of *pure metals*, and finally

(3) attenuation of *shear* ultrasonic waves in the rods of *pure* metals.

The grouping appears all the more reasonable, since the structure of steels is more difficult to model theoretically, and since when using shear waves attenuation is easier to measure (the shear wave is nearly parallel to the rod walls and thus on reflection from these walls no mode conversion takes place - [1]). The corresponding data are plotted in Figs 1–3. There and everywhere below we use experimental points only. In figures type a) we present the usual family of curves $\alpha(f)$ parameterized by $D$. In figures type b), we re-plot the data using standard dimensionless variables $D\alpha$ and $D/\lambda$. In figures type c), we re-plot them again using dimensionless variables $v\mathrm{d}\alpha/\mathrm{d}f$ (the differentiation procedure is described in Appendix A) and $D/\lambda$. The straight lines are drawn there to indicate the preferential slope. It is clear that *the universal piece-wise power law* is confirmed for $D/\lambda$. In this respect our results are similar to those based on the generalized Roney theory. Moreover, the considerations offered at the end of the Background section suggest that $D\alpha$ depends on at least one other dimensionless combination involving at least one other spatial scale. We will return to this point below.

It is also clear that $D/\lambda < 1$ for all the analyzed data, and therefore, one would expect at least some of the straight segments lie in the Rayleigh scattering regime. However, the figures type b) show that most measurements are reasonably well described by the second power law (2), with

$$\nu_1 = 2 \tag{7}$$

- for the pure metals as well as steels - even though some data appear to lie in other regimes. In particular, when $D/\lambda < 0.3$, iron rods are best modeled by the fourth power law. The fact that $\nu_1$ is mostly 2 suggests that the scattering law is mostly other than Rayleigh's or that most attenuation is caused by mechanisms other than scattering. This conclusion is rather unexpected.

Even more unexpectedly, *a more powerful universality* emerges if the above data are replotted again, using

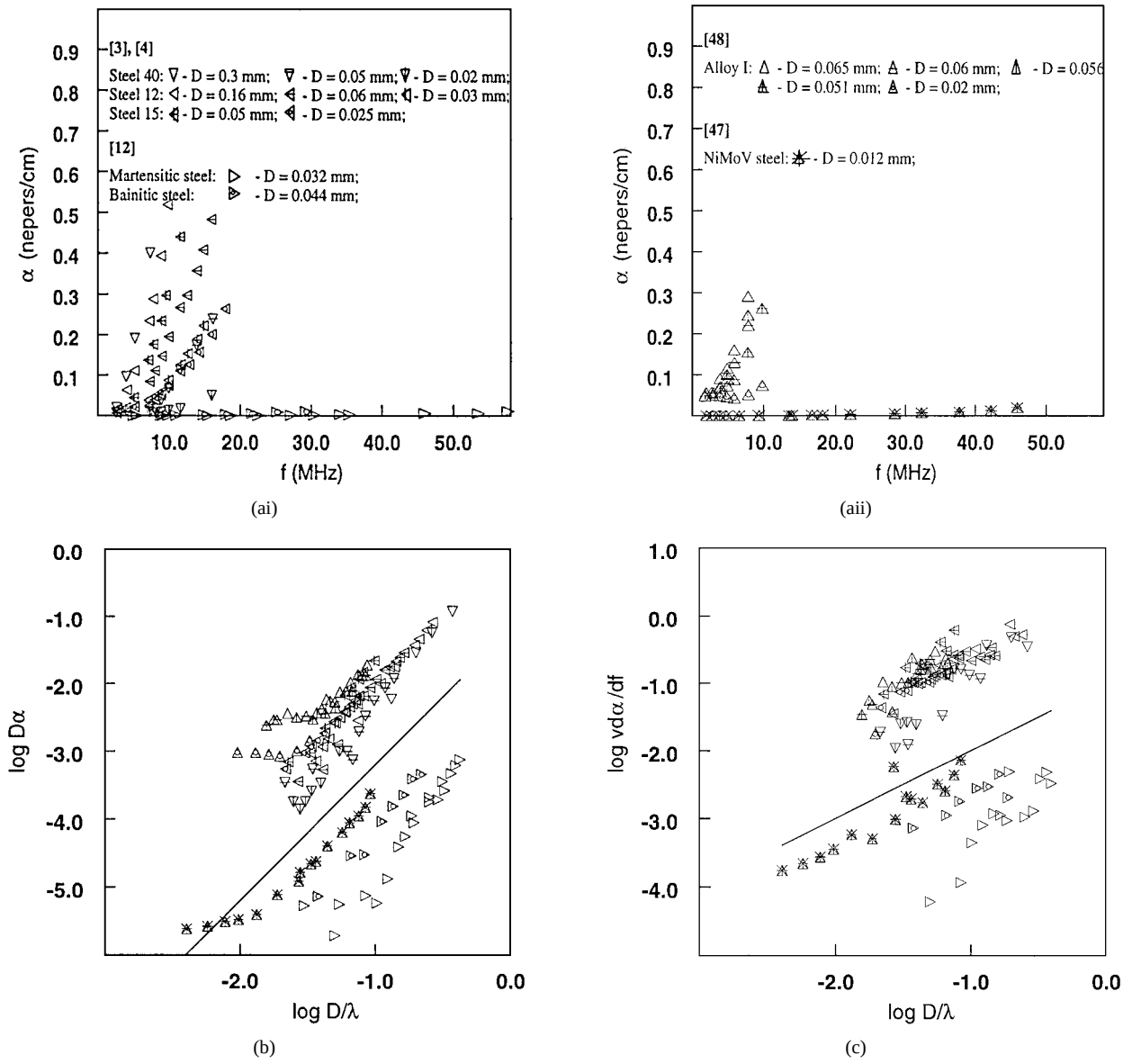


*Figure 1* Attenuation of longitudinal ultrasonic waves in the steel rods: (a) Dependence of $\alpha$ on $f$ according to [3, 4, 12, 47, 48]; (b) Dependence of $D\alpha$ on $D/\lambda$. The straight line indicates the main slope (2). Its intercept is $-1.2$. (c) Dependence of $v\mathrm{d}\alpha/\mathrm{d}f$ on $D/\lambda$. The straight line indicates the main slope (1). Its intercept is $-1$.

Equation 6, so that the variables are $v\mathrm{d}\alpha/\mathrm{d}f$ and $D\alpha$. This particular *model structure* had been arrived at via exploratory data analysis which involved testing various *equivalent* versions of the piece-wise power law hypothesis. It allows a *convenient* data visualisation, i.e. reduction in visual data spread, and thus leads to smaller variance of residuals. The resulting diagrams for longitudinal and shear waves are presented in Figs 4a and 5a respectively. Here all data for both steels and pure metals are utilized. One could attempt to fit these data using the ordinary linear regression and choosing $v\mathrm{d}\alpha/\mathrm{d}f$ as the regression variable. Then we have

$$\nu_0 = 1 \pm 3\%, \quad \log A_0 = -1.4 \pm 3\%, \quad q = 0.89, \tag{8}$$

where $q$ is the correlation coefficient. It is important to choose $v\mathrm{d}\alpha/\mathrm{d}f$ as the regression variable because linear regression gives unbiased estimates only under the assumption that the regression variable is known exactly, the regression parameters are constant and the error on the dependent variable is zero mean and normally distributed. Even with the above choice, these conditions may be violated: Indeed, the resulting straight line which is shown in Figs 4b and 5b corresponds to $\nu_0 = 3/4$, that is the fourth power law, $\nu_1 = 4$. However, the graphs of type b) presented in Figs 1–3 show that *when data for different materials are fitted separately*, in most experiments under consideration the predominant regime is different to Rayleigh's. It is the scrambling of the data (which masks the parameter variation from one group of materials to another) that produces the illusion of the Rayleigh law. Thus, the fitting which does not involve testing the assumptions underlying the linear regression algorithm confuses the physics.

A more refined approach is to use the data compartmentalization as presented in Figs 1–3 and gives the value of $\nu_1 = 2$ (see (7)). This suggests that

$$\nu_0 = 0.5 \tag{9}$$

Using this insight we can identify the two segments presented in Figs 4a and 5a by re-grouping the data again, now into *two* classes of materials:

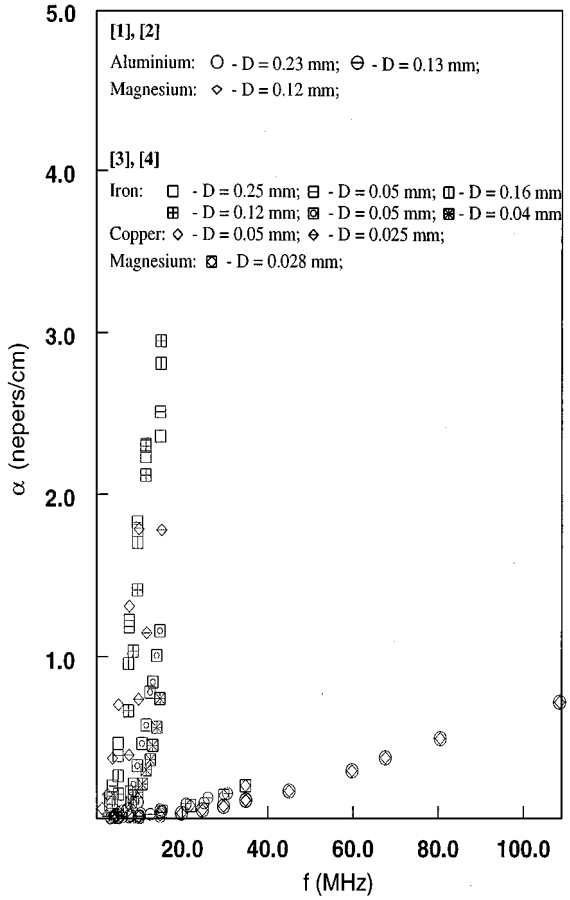


(a)

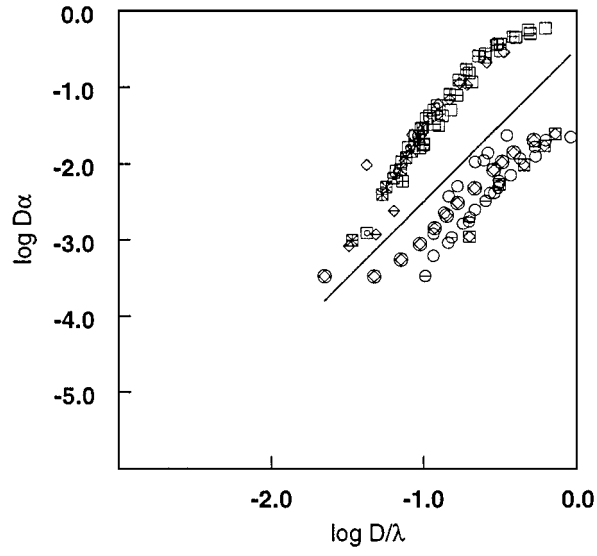


(b)

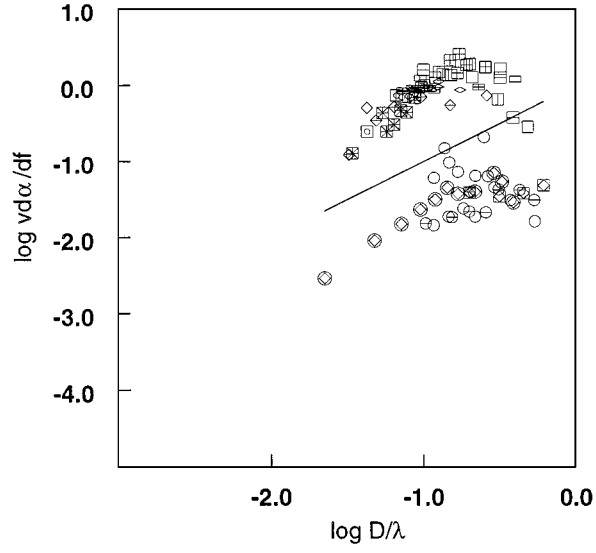


(c)

*Figure 2* Attenuation of longitudinal ultrasonic waves in the rods of pure metals: (a) Dependence of $\alpha$ on $f$ according to [1–4]; (b) Dependence of $D\alpha$ on $D/\lambda$. The straight line indicates the main slope (2). Its intercept is $-1.2$. (c) Dependence of $v\mathrm{d}\alpha/\mathrm{d}f$ on $D/\lambda$. The straight line indicates the main slope (1). Its intercept is $-1$.

(1) those for which $\log v\mathrm{d}\alpha/\mathrm{d}f > -1.5$, and
(2) those for which $\log v\mathrm{d}\alpha/\mathrm{d}f < -1.5$.

Of course, this type of grouping is *consistent* with the earlier representations, given in Figs 1–3. These show that in the materials of the second group the attenuation itself is very low; their generalized material constant $A$ is very small. Note that the materials in question are the NiMoV steel used in [47], martensitic and bainitic steels used in [12], and aluminum and magnesium used in [1–4]. The fact that different authors produce similar results for magnesium rods suggests that we are dealing with genuine differences in material properties rather than differences in experimental procedure.

Finally, the visual inspection of Figs 1b, 2b and 3b shows that not all the data in those classes are described by the second power law, other regimes are present as well at lower and higher values of $v\mathrm{d}\alpha/\mathrm{d}f$. Selecting those that are and performing the fitting, we obtain for the smaller attenuations

$$\nu_0 = 0.6 \pm 1\%, \quad \log A_0 = -1 \pm 5\%, \quad q = 0.99. \tag{10}$$

and for the larger,

$$\nu_0 = 0.6 \pm 5\%, \quad \log A_0 = 1 \pm 5\%, \quad q = 0.99. \tag{11}$$

The above correlation coefficients are higher than in (8). The values of $\nu_0$ are close to (9), particularly, if it is taken into the account that the estimates of standard deviation in parameters are sensitive to error distribution and thus, are not very reliable (they also deteriorate with decreasing number of observations). The fact that the differences in the generalized material constant do not appear large within each group may be explained by comparing (3) to (4). We can see that when using the log-log scale, the last formula leads to halving of the differences in intercepts.

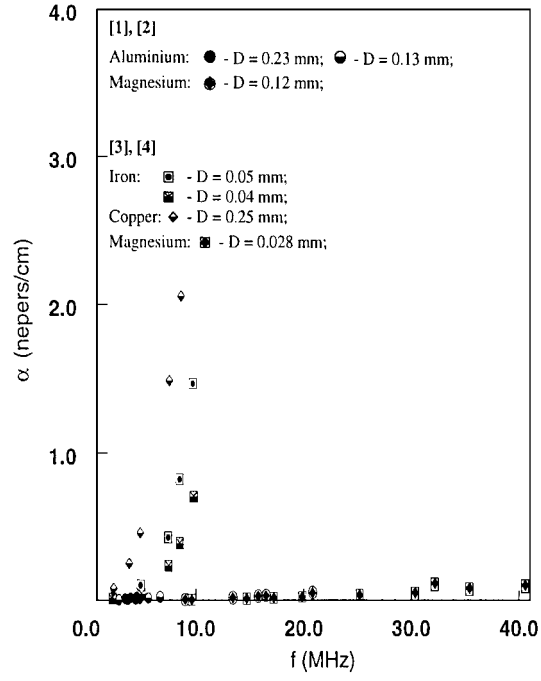


(a)

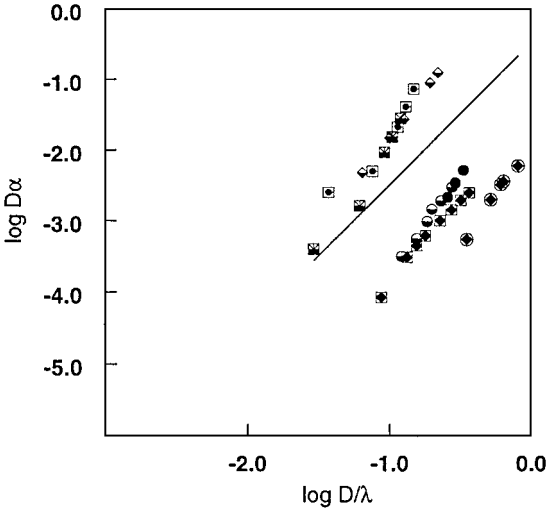


(b)

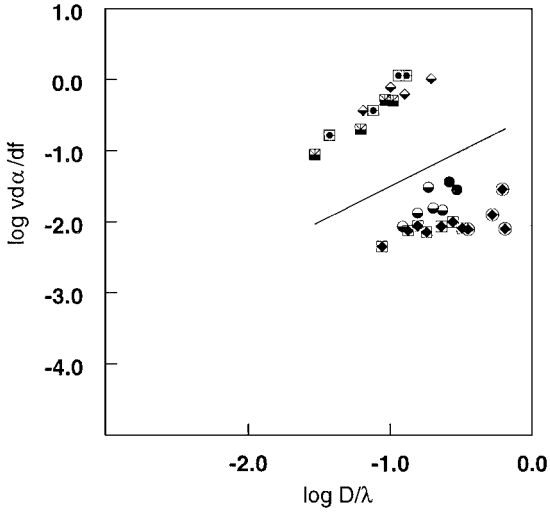


(c)

*Figure 3* Attenuation of shear ultrasonic waves in the rods of pure metals: (a) Dependence of $\alpha$ on $f$ according to [1–4]; (b) Dependence of $D\alpha$ on $D/\lambda$. The straight line indicates the main slope (2). Its intercept is $-1.2$. (c) Dependence of $v\mathrm{d}\alpha/\mathrm{d}f$ on $D/\lambda$. The straight line indicates the main slope (1). Its intercept is $-1$.

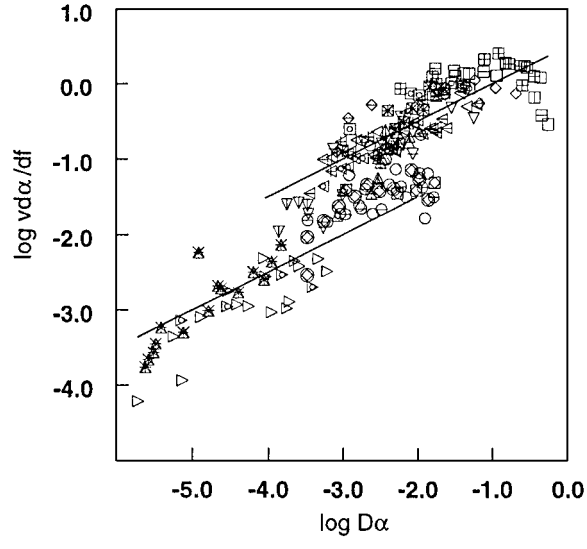


(a)

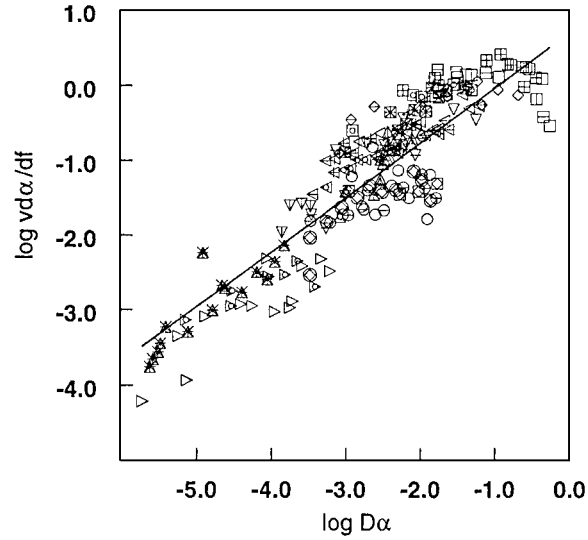


(b)

*Figure 4* Dependence of $v\mathrm{d}\alpha/\mathrm{d}f$ on $D\alpha$ for longitudinal waves in metal rods: (a) The slope of the straight lines is 0.5 and the intercepts are $-0.5$ and 0.5 respectively: (b) The slope of the straight line is 0.75 and the intercept is 0.8. The correlation co-effiecient is $q = 0.8$.

There is an interesting analogy with the fracture mechanics: It has been known for a long time that for any given material the family of curves describing the relationship between the length of fracture $\ell$ and the number of loading cycles $N$ which is parameterized with the maximum magnitude of cyclic load $\sigma$ may be re-plotted as one universal graph or master curve when variables $\mathrm{d}\ell/\mathrm{d}N$ and intensity factor $\Delta K \equiv \sigma\sqrt{\ell}$ are used (see Fig. 6). It transpires that in both fracture mechanics and ultrasonic inspection, a universal representation is achieved by plotting a "kinetic" variable which represents the rate of change of the main measured quantity ($\mathrm{d}\ell/N$ or $\mathrm{d}\alpha/\mathrm{d}\lambda^{-1}$ respectively) versus the product of a power of the main measured quantity ($\ell^{1/2}$ or $\alpha$ respectively) and a parameter which is specific to the experiment ($\sigma$ or $D$ respectively). In both situations major portions of the master curve are well described by power-type laws. Most applications in fracture mechanics rely on the kinetic diagram with only *one* major linear portion. Similarly to our case, the presence

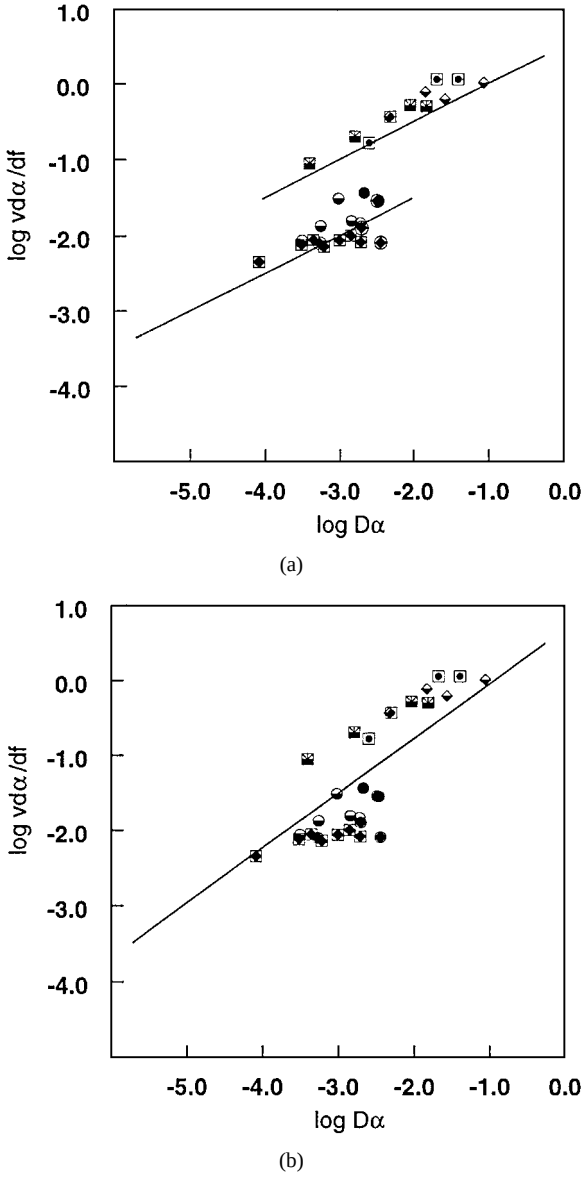


*Figure 5* Dependence of $v\mathrm{d}\alpha/\mathrm{d}f$ on $D\alpha$ for shear waves in the metal rods. (a) The slope of the straight lines is 0.5 and the intercepts are $-0.5$ and 0.5 respectively; (b) The slope of the straight line is 0.75 and the intercept is 0.9. The correlation coeffiecient is $q = 0.9$.

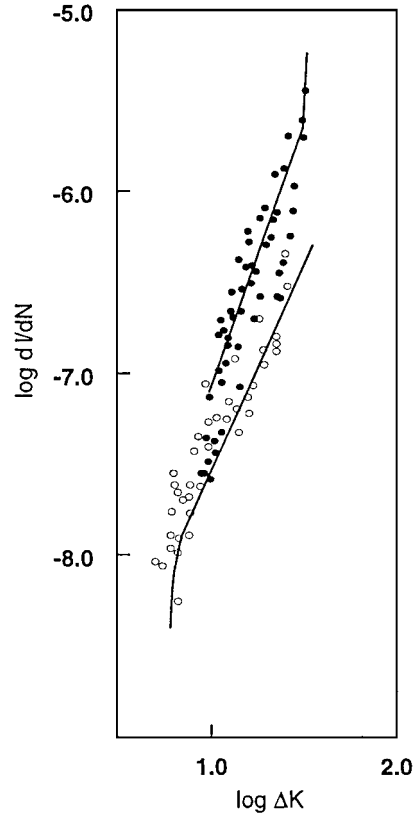


*Figure 6* Kinetic damage diagram: $\ell$(m) is the length of a micro-crack, $N$ the number of load cycles and $\Delta K \equiv \sigma\sqrt{\ell}$ (MPa$\sqrt{\mathrm{m}}$) is the change in the stress intensity factor. A copy of Fig. 2 in [49].

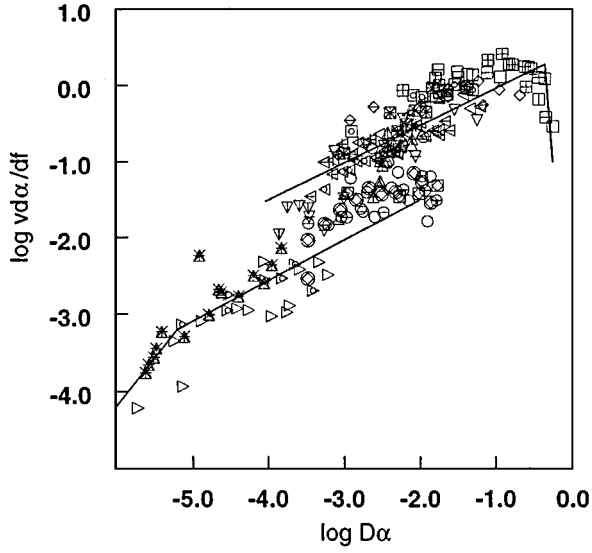


*Figure 7* Dependence of $v\mathrm{d}\alpha/\mathrm{d}f$ on $D\alpha$ for longitudinal waves in metal rods, with indication of other possible regimes.

of *two* such portions becomes apparent only on testing a large number of samples and statistical data analysis supported by analysis of damage mechanisms [50].

To conclude, most of the $\alpha(f, D)$ data from the original three classes can be described by using just two straight lines, one for higher attenuation per unit frequency, and one for lower. It is quite clear that the data points which have been obtained using the longitudinal waves and which fall off these lines can be easily identified from Figs 1b, 2b or 3b as belonging to other than the predominant $D/\lambda$ regimes. In Fig. 7 we present the fuller master curve which emphasizes the presence of more than just two major linear portions. Too few data points have been obtained using the shear wave experiments to confirm that they are indeed more precise, and to check whether they also fall into different $D/\lambda$ regimes. However, it is clear that the two straight segments represented in Figs 4a and 5a describe both types of waves equally well.

## 4. Practical application of the new approach

It is easy to see that given a rod of a polycrystalline material and $\alpha(f)$ data covering a range of frequencies, the master curve presented in Fig. 4a can be used to establish the mean grain size of this material. Indeed, all we have to do is apply the following procedure:

1. Assume speed of propagation (this is much less sensitive to microstructure than attenuation). Assume $D = 0.3$ mm.

2. Plot $\log v\mathrm{d}\alpha/\mathrm{d}f$ vs $\log D\alpha$ using the assumed values of $v$ and $D$.

3. Establish whether the above plot contains the $f^2$-portion, where the slope is $\nu_0^{-1} = 2$.

4. If yes, translate it horizontally to fit the master curve; choose a point which lies on both the translated plot and the master curve, and use the corresponding $v\mathrm{d}\alpha/\mathrm{d}f$- and $\alpha$-values to identify the mean grain size $D$.

It is also easy to check by inspection of Figs 4a and 5a that this procedure may produce a very high level of accuracy; an error of 10–20% rising to 100% for the lower mean grain sizes (the iron data with $D < 0.3$ mm should not be taken into account, since as we mentioned above, these data appear to be consistent with the hypothesis of Rayleigh's scattering). Let us illustrate this by justifying the last figure. Indeed, comparing predictions based on the master curve to the measured values, the maximum error in $\log D\alpha$ is

$$\log(D\alpha)_{\text{predicted}} - \log(D\alpha)_{\text{measured}} \approx 0.3, \qquad (12)$$

which implies that for an accurately measured $\alpha$, the maximum relative error in $D$ is

$$\frac{D_{\text{predicted}}}{D_{\text{measured}}} \approx 2. \qquad (13)$$

More accurate figures could be obtained if we had, borrowing the neural networks terminology, a larger training and a large testing set. Thus, our accuracy is comparable with that reported in [51] - without having to adhere to the Rayleigh regime or choose a standard specimen (cf. [12]). In some cases the accuracy may be even as high as that reported in [52] where a much more elaborate schedule is advocated. We believe that in most cases it cannot deteriorate by much. Indeed, a careful study of the data published in [53] shows that our generalized material constants are very close to the stochastic scattering factors. For example, the value for this factor for aluminum is 0.005, which is consistent with the corresponding intercept of $-1.6$ in Fig. 2b. Similarly, for copper this factor is about 44 times higher, again in accordance with Fig. 2b. With the exception of Tungsten and lead, all other metals mentioned in [53] fall into the identified two groups. This leads us to believe that the majority of metals should be described by our master curve well. By the same token if a specimen under test exhibits an excessively high (over 1) or excessively low (under 0.001) value of $|v\mathrm{d}\alpha/\mathrm{d}f|$ this would indicate that using our master curve does not have to give reliable results.

## 5. Conclusions

It has been shown that practically all published ultrasonic data pertaining to attenuation of ultrasonic waves in polycrystalline materials, both pure metals and alloys, may be described by one master curve, an universal piece-wise linear graph which represents a relationship between two dimensionless variables, $\log D\alpha$ and $\log v\,\mathrm{d}\alpha/\mathrm{d}f$ and is described by the following equation

$$\log D\alpha = \begin{cases} 2\log v\dfrac{dd}{df} + 1 & \text{if } \log v\dfrac{dd}{df} < -1.5, \\ 2\log v\dfrac{dd}{df} - 1 & \text{if } \log v\dfrac{dd}{df} > -1.5. \end{cases} \qquad (14)$$

Although it cannot be proven that all the new data will always exhibit the same behavior it seems remarkable that practically all the data we could find do. This suggests that the above graph has immediate practical applications:

(1) Its independence of the material is a novel and useful feature, since it does not appear feasible to establish universal threshold values which separate the traditional attenuation regimes (see Tables II and III). In particular, different ratios between material constants used in Table II would produce different thresholds. These might also vary with the minimum and maximum grain size $D_{\min}$ and $D_{\max}$.

(2) It has been shown that the master curve may be employed to estimate the mean grain size $D$ using ultrasonic attenuation measurements, without recourse to standard specimens or measurements of material constants. The standard deviation in the mean grain size is estimated to be 10–20%, rising to 100% at the lower mean grain sizes. Excessively high (over 1) or excessively low (under 0.001) values of $|v\mathrm{d}\alpha/\mathrm{d}f|$ would indicate that the procedure does not have to give reliable results.

(3) The metallographic techniques for measurement of the mean grain size are a subject of much controversy. The proposed graph might be used as an additional argument when validating the metallographic measurements of this nature.

From the fundamental point of view our results appear interesting as well: The slope of the linear portions of the master curve is consistent with $D\alpha$ being proportional to the second power of $D/\lambda$ for all materials but iron, even though the data lie in the parameter range where Rayleigh's scattering is expected. The frequent occurence of the second power law in steels has been noted in [17] before: it is remarked even in [2] that the data on aluminum with grain size 0.23 mm could be fitted rather well using the square law; and we have discovered a similar situation when working with ceramics data [54]. However, the predominance of this law has never been spelled out before. The law can be due to several different physical mechanisms, stochastic scattering, a particular grain size distribution, dislocation damping, molecular relaxation at a frequency above the experimental range, thermo-elastic loss etc. Since most authors believe that in the megahertz regime absorption effects are neglible, this narrows the problem down to the model of scattering or the grain size distribution which follows a power law (see the above-mentioned results obtained in [44, 45]). However, it seems unlikely that all grain distributions may be thus

described. Moreover, the power-law distributions do not automatically imply additional characteristic scales and our results presented in Figs 1c, 2c, and 3c suggest that an extra spatial scale is involved.

Thus, it is likely that it is the multiple scattering involving one extra spatial scale that prevails. The hypothesis is further confirmed by studying the data published in [53] and discussed at the end of the last section. Although the formulas for the stochastic scattering factors do not exhibit dependence on other scales, a weak dependence of this nature is likely, say, if the assumption (v) is relaxed and the correlation length characterizing the autocorrelation function for the scattered field is introduced. This is particularly plausible because the stochastic scattering model often underestimates the level of scatter by as much as a factor of 2 (*ibid*). Unfortunately, at present there appears to be no better than the stochastic scattering model description of multiple scattering by closely packed strong scatterers against which our conclusion may be easily tested.

Finally, the fact that two different groups of data emerge does not imply that there are no differences within the groups, only that these differences are not particularly pronounced. Indeed, we have shown that comparing (3) to (4) and using the log-log scale, the last formula leads to halving of the differences in intercepts. The confirmation or refutation of the multiple scattering hypothesis may be obtained only on carrying out a series of carefully planned experiments, covering a wide range of frequencies, materials and microstructures.

## Appendix A

Let us briefly discuss our differentiation procedures.

As we have mentioned already, the difference between attenuations experienced at neighboring frequencies is the main quantity measured in attenuation experiments. However, this type of data are not easily available, and the typical published curves represent the $\alpha(f)$ dependence as in Figs 1a, 2a and 3a. Consequently, numerical differencing procedures have been employed to compute $\mathrm{d}\alpha/\mathrm{d}f$. To establish robustness of our results two such procedures have been tried: the straightforward differencing and a more sophisticated method based on the assumption that $\alpha$ is a monotonically increasing function of $f$. This particular constraint allows us to use a relatively fast optimization algorithm developed in [55]. (1981) to find $\delta\alpha_i$'s which minimize the following cost function

$$J_0 \equiv \sum_{i=0}^{N-1}\left[\alpha_{i+1} - \sum_{n=1}^{N-1}\delta\alpha_n H(i-n)\right]^2 + \beta^2 \sum_{n=1}^{N-1}\delta\alpha_{n+1}^2. \tag{A.1}$$

Here $\alpha_{i+1} = \sum_{n=1}^{i}\Delta\alpha_n = \sum_{n=1}^{N-1}\Delta\alpha_n H(i-n)$; $\Delta\alpha_n \equiv \alpha_{n+1} - \alpha_n$; $H(j)$ is the discrete Heaviside function; $\sum_{n=1}^{0}\delta\alpha_n \equiv 0$; $N$ is the number of available discrete points and all the data are shifted, so that $\alpha_1 = 0$. This algorithm is incorporated into our EDA (Exploratory Data Analysis) package as a DECOP subroutine (for DECOnvolution with Positive kernels). When the optimization procedure is carried out for

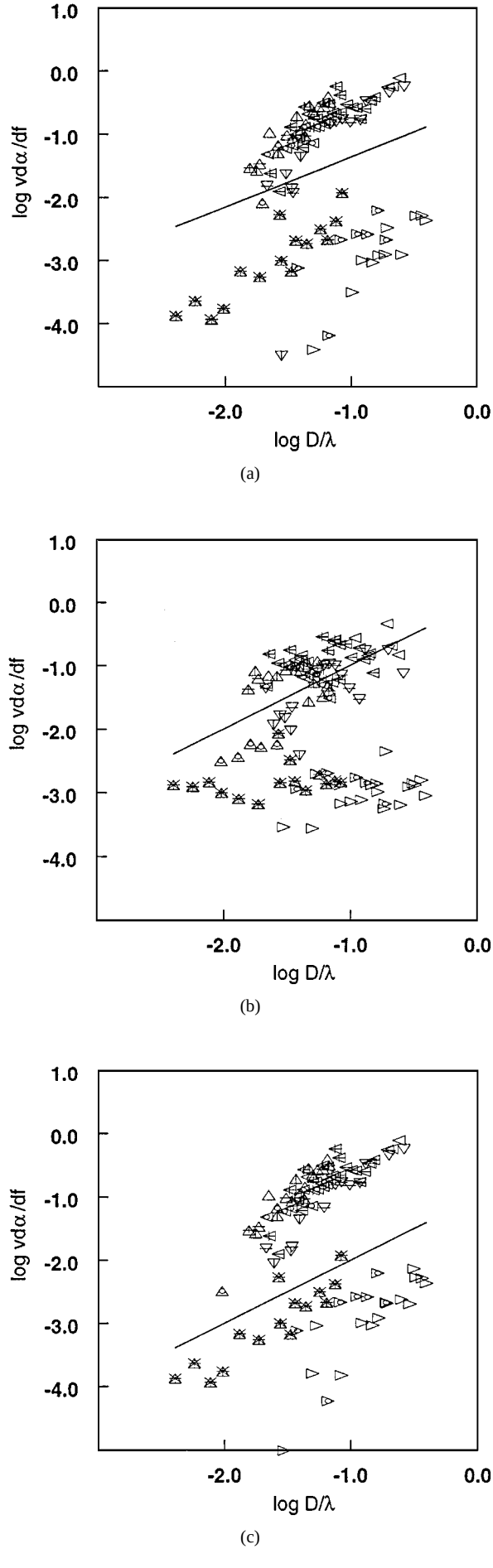


*Figure A1* The rate of ultrasonic attenuation $v\mathrm{d}\alpha/\mathrm{d}f$ as estimated using (a) DECOP with $\beta^2 = 10^{-4}$, (b) DECOP with $\beta^2 = 10$, and (c) the finite-differencing technique. The key and parameters of the straight line as in Fig. 1c.

each value of the frequency counter $i$, $(\mathrm{d}\alpha/\mathrm{d}f)_i$ is estimated to be $\delta\alpha_i/\delta f_i$, where $\delta f_i = f_{i+1} - f_i$. Thus, even though the original algorithm has been developed for an evenly spaced discrete argument we can deal with the discrete function $\alpha(f)$ for which the values of $f$ are unevenly spaced. The results depend on $\beta^2$ but weakly: Two different estimates of the attenuation derivative corresponding to two different values of $\beta^2$ are presented in Fig. A1a and b. It is clear that for small values of $\beta^2$ which give more weighting to the first, variance, term in (A.1) the result is practically indistinguishable from the one obtained using the straightforward differencing (Fig. A1c). Larger values of $\beta^2$ give more weight to the second term in (A.1) which is the $L_2$-norm of $\delta\alpha$. In the main body of the paper we choose $\beta^2 = 0.5$ (see Fig. 1c) which corresponds to mild smoothing of the $\alpha(f)$ curves. The choice achieves a trade-off between two conflicting requirements: on the one hand, there is a perceptible difference between the outcomes of our two differentiation procedures; on the other hand, the dominant slope is $\approx$1 (since it is $\approx$2 in Figs 1b, 2b and 3b). Interestingly, the final estimates obtained using the two differentiation procedures differ mainly in their initial values, where as a rule, the measurement precision is at its lowest and the beam spreading prevails. Other differentiation procedures involving prior smoothing could be utilized, but it was not felt necessary to introduce this extra degree of refinement.

## Acknowledgements

The first author carried out part of this work in her capacity of an Ex-Quota Fellow and gratefully acknowledges the U.K. Royal Society grant. We are also indebted to John Evans for allowing us to use his TESLA package to tabulate data published in the graphic form. Our own graphics have been produced using a FORTRAN 77/PS package originally developed by Stuart Dahl and Andrew Gilbert and now incorporated into our EDA package.

## References

1. W. P. MASON and H. Y. MCSKIMMIN, *J. Acoust. Soc. Am.* **19**(3) (1947) 464.
2. *Idem., J. Appl. Phys.* **19** (1948) 940.
3. L. G. MERKULOV, *Zh. Tekh. Fiz.* **26** (1956) 64. (English trans.: Sov Phys-Tech Phys, vol. 1, pp. 59–69).
4. *Idem., ibid.* **27**(6) (1957) 1386. (English trans.: Sov. Phys.-Tech. Phys., vol. 2, pp. 1282–1286).
5. R. W. ARMSTRONG, *Metall. Trans.* **1** (1970) 1169.
6. *Idem.*, "Advances in Material Research, Vol. 4" (Interscience, New York, 1970) p. 101.
7. E. O. HALL, "Yield Point Phenomena in Metals and Alloys" (Plenum Press, New York, 1970).
8. G. I. BARENBLATT, "Dimensional Analysis" (Gordon and Breach, New York, 1987).
9. C. F. YING and R. TRUELL, *J. Appl. Phys.* **27** (1956) 1086.
10. LORD J. W. S. RAYLEIGH, "Theory of Sound, Vol. 2" (Macmillan Co., New York, 1929) p. 152.
11. E. P. PAPADAKIS, *J. Acoust. Soc. Am.* **37** (1965) 703.
12. *Idem., ibid.* **32**(12) (1960) 1628.
13. H. B. HUNTINGTON, *ibid.* **22**(3) (1950) 362.
14. B. BRIDGE, in "Trends in NDE Science and Technology: Proc. 14th World Conf. on NDT, New Delhi, India," edited by C. G. Krishnadas Nair, Baldev Raj, C. R. L. Murty and T. Jayakumar (Oxford & IBH Publishing Co., New Delhi, 1996) p. 2217.
15. W. ROTH, *J. Appl. Phys.* **19** (1948) 901.
16. E. M. LIFSHITS and G. D. PARKHOMOVSKII, *Zh. Eksper. i Teor. Fiz.* **20** (1950) 175.
17. E. P. PAPADAKIS, *J. Appl. Phys.* **35**(5) (1964) 1474.
18. L. RODERICK and R. TRUELL, *ibid.* **23** (1952) 267.
19. E. P. PAPADAKIS, *J. Acoust. Soc. Am.* **31** (1959) 150.
20. *Idem., ibid.* **40** (1966) 863.
21. *Idem.*, in "Nondestructive Methods for Material Property Determination," edited by C. O. Ruud and R. E. Green (Plenum, New York, 1984) p. 151.
22. S. SERABIAN and R. S. WILLIAMS, *Mater. Eval.* **36**(8) (1978) 55.
23. J. F. BUSSIÈRE, "Applications of NDE to the processing of metals," *Rev. Prog. Quant. NDE.* **6B** (1987) 1377.
24. H. KOLSKY, "Stress Waves in Solids" (Dover Publications, 1953).
25. R. W. WEGEL and H. WALTHER, *Physics* **6** (1935) 141.
26. R. BECKER and W. DOERING, "Ferromagnetismus" (Springer Verlag, Berlin, 1939) (in German).
27. W. P. MASON, *Phys. Rev. Lett.* **83** (1951) 683.
28. *Idem., Rev. Mod. Phys* **25** (1953) 136.
29. J. S. KOEHLER, "Imperfections in Nearly Perfect Crystals" (John Wiley, New York, 1952).
30. A. V. GRANATO and K. LÜCKE, *J. Appl. Phys.* **27** (1956) 583.
31. *Idem., ibid.* **27** (1956) 789.
32. K. F. HERTZFELD and T. A. LITOVITZ, "Absorption and Dispersion of Ultrasonic Waves" (Academic Press Inc., New York: 1959) Ch. 2.
33. W. J. BRATINA, U. M. MARTIUS and D. MILLS, *J. Appl. Phys.* **31** (1960) S241.
34. U. M. MARTIUS and W. J. BRATINA, *ibid.* **32** (1961) 280S.
35. C. ZENER, *Phys. Rev. Lett.* **52** (1937) 230.
36. *Idem., ibid.* **53** (1938) 90.
37. E. E. ALDRIDGE, in "Non-Destructive Testing: Views, Reviews, Previews," edited by Egerton (Oxford University Press, Glasgow, 1969) p. 31.
38. J.-P. MONCHALIN and J. F. BUSSIÈRE in "Nondestructive Methods for Material Property Determination," edited by C. O. Ruud and R. E. Green (Plenum, New York, 1984) p. 289.
39. *Idem., Rev. Prog. Quant. NDE* **IVB** (1985) 965.
40. F. BERGNER and K. POPP, *Scripta Metallurgica et Materiala* **24** (1990) 1357.
41. R. K. RONEY, Ph.D. thesis, California Institute of Technology, 1950.
42. C. L. PEKERIS, *Phys. Rev.* **71** (1947) 268. Erratum 457.
43. D. W. NICOLETTI and D. KASPER, *Rev. Prog. in Quant. NDE* **13B** (1994) 1729.
44. D. W. NICOLETTI and A. ANDERSON, *J. Acoust. Soc. Am.* **101**(2) (1997) 686.
45. D. W. NICOLETTI and D. KASPER, IEEE Trans. Ultras. Ferroelec. Freq. Control **41**(1) (1994) 144.
46. K. J. ÅSTRÖM and P. EYKOFF, *Automatica* **7** (1971) 23.
47. S. SERABIAN, *Br. J. Non-Destr. Test* **22**(2) (1980) 69, 73, 76.
48. R. KLINMAN, G. R. WEBSTER, F. J. MARSH and E. T. STEPHENSON, *Mater. Eval.* **38** (1980) 26.
49. L. R. BOTVINA, A. I. DANILOV and I. B. OPARINA, *Problemy Prochnosti* **1** (1990) 14.
50. L. R. BOTVINA, "Kinetics of Fracture of Construction Materials" (Nauka, Moscow, 1989) (in Russian).
51. E. P. PAPADAKIS, *J. Acoust. Soc. Am.* **37** (1965) 711.
52. H. WILLEMS and K. GOEBBELS, *Met. Sci.* **15** (1981) 549.
53. E. P. PAPADAKIS, *J. Acoust. Soc. Am.* **43**(4) (1968) 876.
54. L. R. BOTVINA, L. FRADKIN and B. BRIDGE, *Non-Destructive Testing and Evaluation* **12** (1995) 103.
55. J. P. BUTLER, J. A. REEDS and S. V. DAWSON, *SIAM J. Numer, Anal.* **18**(3) (1981) 381.

*Received 13 May 1999*
*and accepted 1 February 2000*